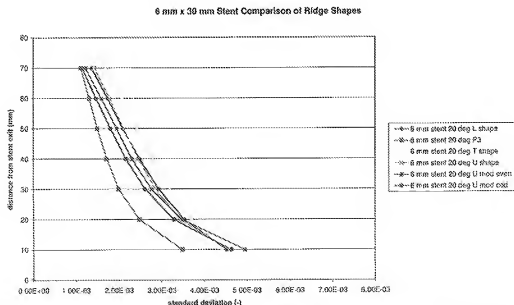


## DECLARATION

I, Dr Graeme Houston hereby declare as follows:

1. I am a co-inventor of US patent application serial no. 10/562471. My curriculum vitae is annexed to this declaration.
2. I have been responsible for a series of experiments to compare the effect of different profile shapes of a spiral inducer on spiral flow within vascular grafts and stents.
3. Several experiments were carried out in order to determine the optimum profile shape for a ridge (the spiral inducer), as set out in Annexes A & B. In these experiments different profile shapes were tested, such as asymmetric ("P3"), U, T & L profile shapes. From these investigations, it was concluded that the asymmetric (P3) shape is an advantageous profile shape compared with the others.
4. A parametric study was carried out using STAR-CD software to compare the computational fluid dynamics modelling of spiral flow induction (swirl number) and pressure drop through various stents as described in Annex A. This study was performed using stents, but it is expected that equivalent results would be obtained using alternative vascular conduits, such as grafts or stent grafts. The asymmetric P3 profile consistently showed the lowest standard deviation over the downstream length of the stent out of all the profiles tested, which is indicative of an even, smooth spiral flow pattern on the axial plane. The P3 profile also provided the lowest pressure drop along the length of the conduit, which is indicative of the fluid pressure being maintained along the length of the conduit. Overall, the results obtained for swirl number, standard deviation and pressure drop show that the asymmetric P3 shape is the optimal shape for the ridge profile.
5. The following graphs are a summary of the results; further results are shown in Appendix 1.

Figure 33: 6 mm Stent Comparison of Ridge Shapes; Swirl Number



Lower (optimal) standard deviation is seen for the P3 (asymmetrical) shape compared to the T, U & L shapes.

Figure 39: 8 mm Stent P3 and U Shaped Profiles

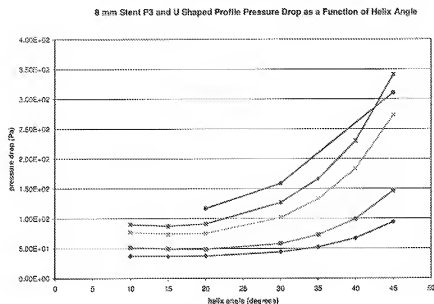
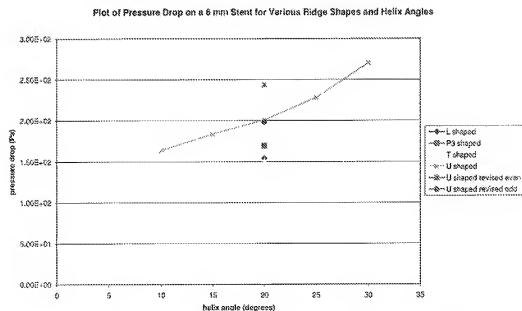


Figure 40: 6 mm Stent Various Ridge Shapes



These graphs show that the P3, L and T shaped ridges resulted in a better pressure drop than a U-shape ridge.

The overall results obtained for swirl number, standard deviation and pressure drop indicate that the asymmetric shape of P3 is optimal for the ridge, in comparison to the other shapes tested.

6. As shown in Annex B, a study was carried out to visually compare the effect of various ridge shapes, namely, P3 (asymmetric), U, T and L shapes, on flow profiles through a stent. The results are shown in Appendix 2, Figs 1-16.

7. The swirl number and standard deviation were also calculated on a plane perpendicular to the flow direction, as explained in Annex B. A higher swirl number indicates greater fluid rotation (swirl) within the conduit. A lower standard deviation indicates that the fluid has a smoother and more coherent swirl pattern. The results are shown in Table 1:

Table 1: Swirl Number and Standard Deviation at 50mm downstream

ridge shape, helix angle	U 30	U 25	U 20	U 15	U 10	T 20	P3 20	L 20
swirl no	0.060262	0.047945	0.0373	0.027568	0.018569	0.042186	0.02707	0.0372
stand dev	0.001578	0.0014	0.001217	0.001016	0.000792	0.001269	0.000953	0.00122

8. The results in table 1 show that the P3 asymmetric profile had a low standard deviation compared with the other shapes tested. This advantageously produces a uniform, smooth fluid swirl pattern and reduces turbulence within the conduit. The P3 20 profile produced a slightly less swirl than the U, T & L 20 ridge shapes, but it gives a more consistent and even swirl pattern due to the lower standard deviation. Therefore, overall, it is a more suitable shape for the ridge profile.

9. The following diagrams summarise the results; additional results are shown in Appendix 2:

Figure 1

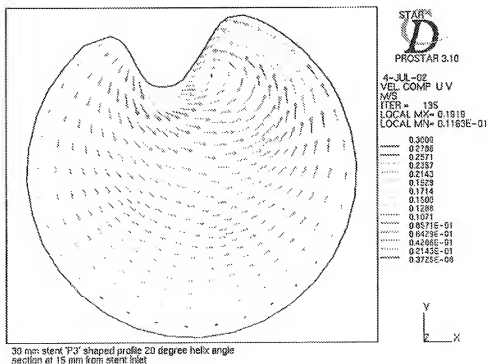
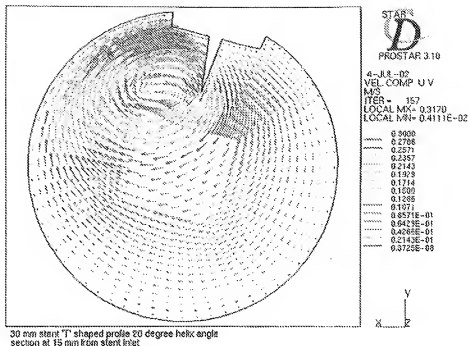


Figure 5



10. The results indicate that the P3 ridge profile causes less marked high velocity ("shedding") on its front or backface compared with the other shapes. Shedding is undesirable in fluid flow through a conduit.

11. In summary, the results demonstrate that an internal formation for a conduit comprising a longitudinally extending member having an asymmetric profile leads to a sufficient swirl number with low standard deviation and a low pressure drop. These results indicate that the asymmetric profile provides good fluid rotation and a smooth, uniform fluid swirl pattern, whilst the fluid pressure is maintained throughout the length of the conduit. Therefore, there is decreased turbulence within the conduit which is desirable for spiral fluid flow through a conduit, especially for blood flow through a stent inserted in a blood vessel, a graft or a stent graft. There was no reason why these results would have been expected prior to carrying out this study.

DR GRAEME HOUSTON

DATED THIS 11th DAY OF MAY 2010

## ANNEX A

A number of stents with varying diameters, lengths, helical angles, number of ridges and spiral inducer shape were chosen for a parametric study. The parameters used to judge the performance of the stents were pressure drop, swirl number and standard deviation of the swirl number.

Three studies were carried out:

- (1) parametric P3 (asymmetric) profile
- (2) parametric triangular profile
- (3) various ridge profiles

### Method

Swirl number has been generally defined as (tangential velocity)/(axial velocity). Static pressure drop was measured across the stent only, not the computational domain.

Four stent diameters were chosen: 3.5 mm, 4 mm, 6 mm and 8 mm. The ridge profile shapes are shown in Figures 1 – 8 in Appendix 1. ***N.B. These Figures are for illustration purposes only.***

#### ***Parametric P3 Profile - 8 mm stent***

A parametric study was carried out using a P3 (Figure 1) profile to investigate the effect of helical angle and graft length on swirl number. Five graft lengths were chosen: 10 mm, 15 mm, 20 mm, 25 mm and 30 mm and each length was modelled with a P3 profile, 2 mm high ridge at the following helical angles: 10°, 15°, 20°, 25°, 30°, 35°, 40° and 45°.

#### ***Parametric Triangular Profile - 3.5 mm and 4 mm stent***

A study was carried out to investigate the effect of a three start triangular ridge of height 1 mm and 0.5 mm at helical angles of 10°, 20°, 30°, 40° and 50°. An initial study was carried out on a 4 mm diameter stent 15 mm long, the ridge was not offset (Figure 2). Further investigation showed that the stent to be used was 3.5 mm in diameter and 16 mm in length. The further study used an offset triangular triple start ridge (Figure 3).

#### ***Various Ridge Profiles - 6 mm stent***

Figures 4 - 6 show further ridge shapes that were tried out namely the 'L', 'T' and 'U' shapes respectively, and later the modified 'U' shape with odd leg lengths and even leg lengths (Figures 7 and 8). A parametric study was carried out on these profiles using a 6 mm diameter stent. Later the 'U' shaped profile was applied to an 8 mm stent.

### **Fluid Properties and Boundary Conditions**

Each model comprised less than 180,000 computational hexahedral cells. No attempt has been made to include the wire cage in the model. The flow was assumed to be laminar, steady state, incompressible and Newtonian, the density and molecular viscosity were taken to be 1050 kg/m<sup>3</sup> and 0.00368 kg/m s respectively. The inlet boundary conditions have been shown in Table 1 below:

diameter (mm)	velocity (m/s)	volume flow rate (ml/s)
3.5	0.316	3
4	0.316	4
6	0.696	20
8	0.696	35

**Table 1: Inlet Boundary Conditions**

The outlet boundary pressure was set to zero in each case and hence the upstream pressure was allowed to float.

### **Results and Discussion**

Each numerical run was completed in under 30 minutes CPU time, the errors falling by three orders of magnitude and field values remained unchanged at the monitoring location. The standard deviation and swirl number were calculated on planes at 10 mm intervals from the end of the graft.

The results have been presented in two ways:

- (1) For each helical angle and graft length, swirl number and standard deviation have been plotted against distance from the downstream stent end. Thus it was easy to compare distances from the end of the stent where the swirl number and/or standard deviation were the same.
- (2) Pressure drop results have been compared on a stent diameter basis.

### Swirl Number and Standard Deviation

#### *Parametric P3 Profile - 8 mm stent*

Consider the swirl number and standard deviation for the P3 profile for an 8 mm stent (Figure 9 - Figure 24). For each helical angle increasing the length of the stent, the swirl number increased as the flow travelled downstream. The standard deviation is also increased with increasing helical angle, but decreased as the flow moved downstream. For the  $10^\circ$ ,  $15^\circ$  and  $20^\circ$  (Figure 9 - Figure 11) helical angle stents there appears to be an increase in swirl number as the flow nears the end of the computational domain. This would be highly unlikely in practice, and can be explained by either it being an end of domain effect as the spiral flow will be quite weak at this point or a numerical convergence problem on that grid. It was likely to be the former as the effect tends to become less as the swirl number increased at this point.

#### *Parametric Triangular Profile - 3.5 mm and 4 mm stent*

For both profiles tested (Figure 2 and Figure 3) in 4 mm and 3.5 mm stents, for helical angles up to  $40^\circ$  for both ridge heights increasing helical angle increases swirl number and standard deviation. The increase in swirl number decreases as helical angle increases. There also appears to be a limiting value of tangential velocity which occurs at about  $40^\circ$  to  $45^\circ$ . Figure 31 shows this clearly i.e. increasing the helical angle reduces swirl number. This could be explained by the flow tripping over the ridge rather than following it, or the tangential velocity may be limited by frictional effects, or a combination of both. In all cases very little spiral flow exists after 70 mm downstream of the stent exit. Clearly the P3 profile is better at producing spiral flow further downstream than the triangular profile c.f. Figure 25, Figure 9, Figure 13, Figure 17 and Figure 24. It is highly probable that this result is scalable to 8 mm as was shown previously by the flow patterns between 8 mm and 4 mm P3 grafts. Hood *et al* (2002)

#### *Various Profiles 6 mm stent*

Figure 4, Figure 5, Figure 6, Figure 7 and Figure 8 show the ridge profiles that have been used in this parametric study. A P3 profile has been used as comparison. For the 6 mm stent ridge shapes have been compared at a helical angle of  $20^\circ$  (Figure 33 and Figure 34), and for the 'U' shaped ridge a comparison has been made at  $10^\circ$ ,  $15^\circ$ ,  $20^\circ$ ,  $25^\circ$  and  $30^\circ$  (Figure 35 and Figure 36). Note that the scales on the swirl number plots are different from the previous plots, this was done in order to capture the more interesting features.

Figure 33 shows that the highest swirl number over the whole downstream length is produced by the 'T' shaped profile. The P3 profile produces the lowest swirl number. All other profiles produced swirl number decay which was similar except the modified 'U' shape with even leg lengths which gave a high swirl number at 10 mm downstream, but decayed very rapidly. Figure 34 shows that the standard deviation of the 'T' shaped profile is greater than all the other profiles at a distance greater than 20 mm downstream of the stent exit and decays almost linearly as the flow moved downstream. This indicated a relatively poor swirl profile on the axial plane as the flow moved downstream. The P3 profile has consistently the lowest standard deviation of all the profiles tested indicating an even spiral flow pattern on the axial plane i.e. the P3 profile produces less swirl than the 'U' profile, but P3 give a more consistent profile.

Figure 35 shows that for a 'U' shaped ridge profile increasing the helical angle increases the swirl number, and it can be seen that for increasing angles up to  $30^\circ$  the rate of change of swirl increases with increasing angle, which was perhaps not apparent with the previous cases (P3, triangular) where helical angles extended to  $45^\circ$  and  $50^\circ$  respectively. Figure 36 shows that increasing helix angle increases standard deviation. For angles up to  $20^\circ$  the standard deviation reduces as expected, but for angles greater than  $20^\circ$  the standard deviation decayed very much more rapidly. This cannot be explained at this time.

Figure 37 shows that when a 'U' shaped ridge was used in an 8 mm stent, increasing the ridge angle increased the swirl number when the helical angle was increased from  $30^\circ$  to  $45^\circ$  the increase in swirl number was disproportionate to the increase in angle from  $20^\circ$  to  $30^\circ$ . This may contradict what has been reported in the previous paragraph. The standard deviation decreased as the flow travelled downstream as expected i.e. spiral flow was dissipated (Figure 38).

### Pressure Drop

Figure 39 shows static pressure drop as a function of helix angle for an 8 mm stent, for both P3 and 'U' shaped ridges.

The P3 and 'U' profile can be curve fit by a third order polynomial of the form:

$$dp = a(ha)^3 + b(ha)^2 + c(ha) + d$$

where: dp is the pressure drop in Pascal and ha is the helix angle in degrees. The residual value is given in column 6.

The coefficients of a, b, c and d are given in the

Length (mm), Profile	a	b	c	d	$r^2$
10 P3	0.0026	-0.1295	2.166	25.658	0.9987
15 P3	0.0045	-0.2187	3.228	35.866	0.9990
20 P3	0.0058	-0.2844	3.6224	48.035	0.9992
25 P3	0.0072	-0.3176	4.4411	56.235	0.9990
30 P3	0.0088	-0.3898	5.8398	60.258	0.9988
30 U	0.0000	0.2401	-7.8758	178.59	1.0000

For a 6 mm stent Figure 40 showed the pressure drop for the various ridge profiles. At a helical angle of  $20^\circ$  the highest pressure drop was exhibited by the revised 'U' shaped profile with even leg lengths. The best pressure drop was given by the 'I' shape.

Similarly to Figure 39, Figure 41 shows static pressure drop as a function of helix angle for a 4 mm and 3.5 mm stent, for both offset and symmetrical triangular shaped ridges.

The triangular profile can be curve fit by a third order polynomial of the form:

$$dp = a(ha)^3 + b(ha)^2 + c(ha) + d$$

where: dp is the pressure drop in Pascal and ha is the helix angle in degrees. The residual value is given in column 6.

The coefficients of a, b, c and d are given in the

$\phi$ (mm), height (mm), Profile	a	b	c	d	$r^2$
4, 1.0, symm	0.0039	-0.1329	2.4255	86.221	0.9999
4, 0.5, symm	0.0007	-0.0146	0.4062	46.735	0.9999
3.5, 1.0, off	0.0060	-0.2113	4.023	129.45	0.9999
3.5, 0.5, off	0.0008	-0.0051	0.4914	65.28	1.0000

Comparison of Figure 39 and Figure 41 shows that for a 15 mm long stent the pressure drop over a triangular ridge was significantly higher when the ridge heights were the same.

### Conclusion

The parametric study carried out using STAR-CD to investigate the effect of flow through various stent configurations showed:

**8 mm P3 profile stent:** For each helical angle, increasing the length of the stent increases the swirl number as the flow travelled downstream. The standard deviation is also increased with increasing helical angle, but decreased as the flow moves downstream.

**4 mm and 3.5 mm stents with symmetrical and offset triangular ridge profiles:** Helical angles up to  $40^\circ$  for both ridge heights, increasing helical angle increases swirl number and standard deviation. The increase in swirl number decreases as helical angle increases. There also appeared to be a limiting value of tangential velocity which occurs at about  $40^\circ$  to  $45^\circ$ , which may be caused by flow tripping over the ridge.

**6 mm stent, with various ridge profiles:** At a helical angle of  $20^\circ$  the highest swirl number over the whole downstream length was produced by the 'T' shaped profile. The 'T' shape also had the worst standard deviation profile. The P3 profile produced the lowest swirl number and standard deviation over the downstream length. In the case of the 'U' shaped ridge for helical angles greater than  $20^\circ$  the standard deviation of the swirl number decays very rapidly, which appeared to be out of step with other cases.

With a 'U' shaped ridge on an 8 mm stent the increase in swirl number was disproportionately large when the helical angle was increased from  $30^\circ$  to  $45^\circ$  than from  $20^\circ$  to  $30^\circ$ . This was contrary to what was expected c.f. P3 profile.

On an 8 mm stent with a P3 and 'U' profile the pressure drop was found to be a function of helix angle and was an excellent curve fit by a third order polynomial. This relationship also applied on the 4 mm and 3.5 mm stents with the triangular profile.

### References

- Hood, R.G. Duff, C. M<sup>c</sup>Leod, H. Sarren, C. and Thomson, A. 2002. Presentation entitled 'R&D presentation3.ppt' 25/6/02 residing in Data\_dirs/presentations.
- Thomson, A. 1999. Analysis of Turbulence Reducing Methods in a Conduit. Tayside Flow Technologies Ltd. Report FD088.
- Thomson, A. 2000. Analysis of Turbulence Reducing Methods in a Conduit Addendum 1. Tayside Flow Technologies Ltd. Report FD089.
- Thomson, A. 2002. CFD Analysis of Inviscid Flow Through an 8 mm Graft. Tayside Flow Technologies Ltd. Report FD012



# APPENDIX 1

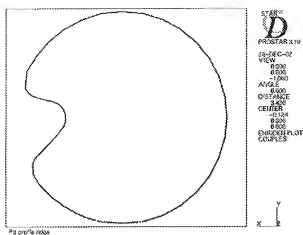


Figure 1

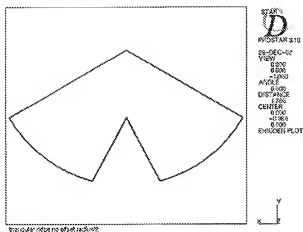


Figure 2

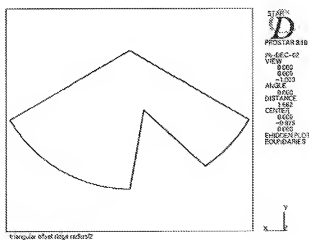
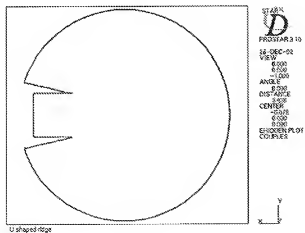
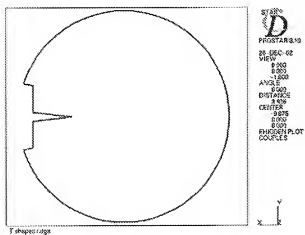
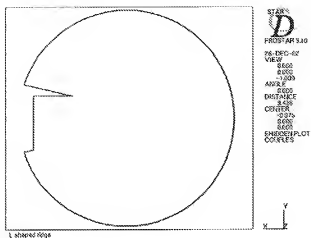


Figure 3



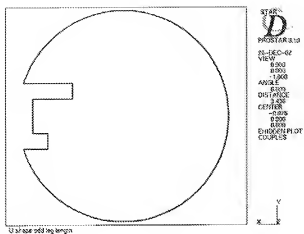


Figure 7

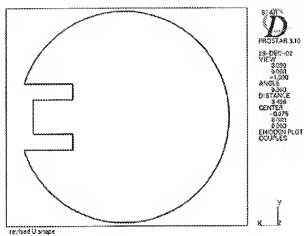


Figure 8

10 Degree Helix Angle Plot of Swirl Number for Various Graft Lengths

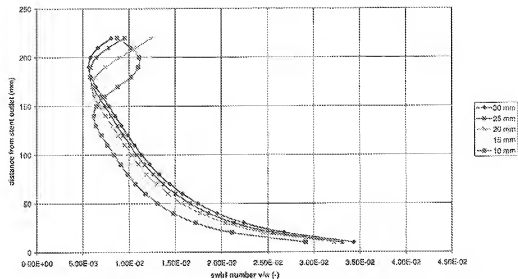


Figure 9: P3 Profile Ridge 8 mm diameter

10 Degree Helix Angle Plot of Standard Deviation for Various Graft Lengths

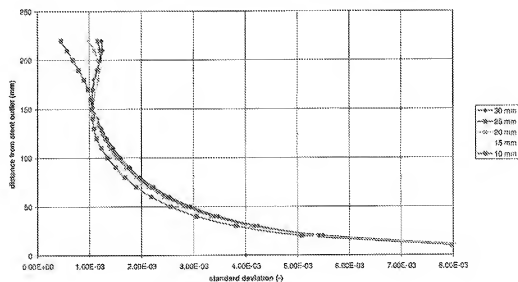


Figure 10: P3 Profile Ridge 8 mm diameter

15 Degree Helix Angle Plot of Swirl Number for Various Graft Lengths

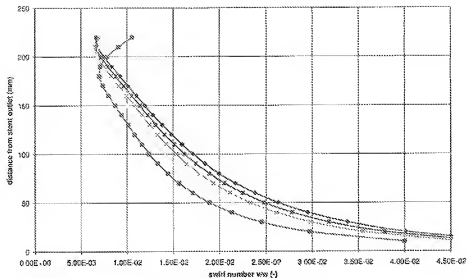


Figure 11: P3 Profile Ridge 8 mm diameter

15 Degree Helix Angle Plot of Standard Deviation for Various Graft Lengths

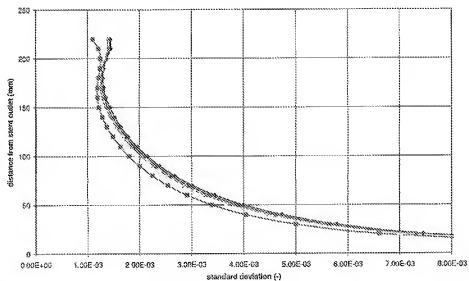


Figure 12: P3 Profile Ridge 8 mm diameter

20 Degree Helix Angle Plot of Swirl Number for Various Graft Lengths

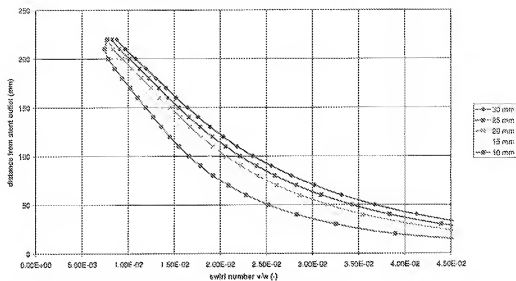


Figure 13: P3 Profile Ridge 8 mm diameter

20 Degree Helix Angle Plot of Standard Deviation for Various Graft Lengths

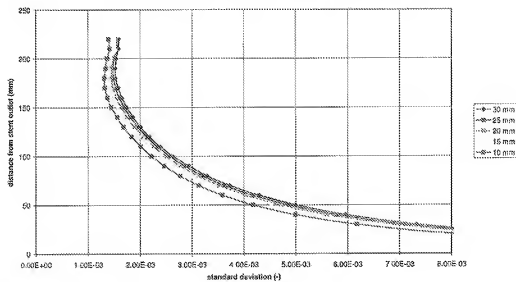


Figure 14: P3 Profile Ridge 8 mm diameter

25 Degree Helix Angle Plot of Swirl Number for Various Graft Lengths

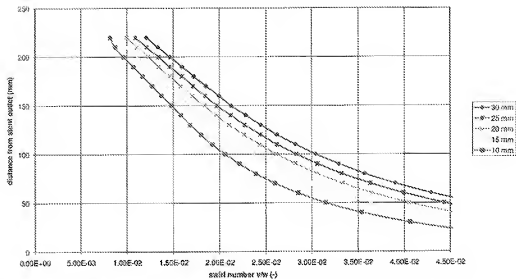


Figure 15: P3 Profile Ridge 8 mm diameter

25 Degree Helix Angle Plot of Standard Deviation for Various Graft Lengths

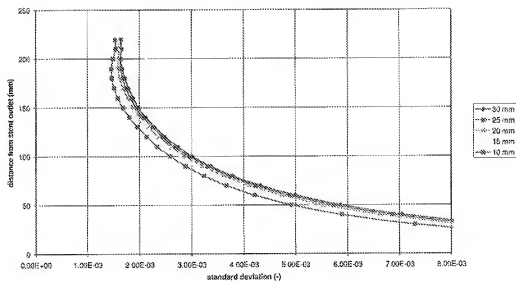


Figure 16: P3 Profile Ridge 8 mm diameter

30 Degree Helix Angle Plot of Swirl Number for Various Graft Lengths

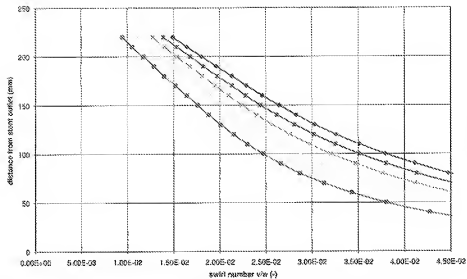


Figure 17: P3 Profile Ridge 8 mm diameter

30 Degree Helix Angle Plot of Standard Deviation for Various Graft Lengths

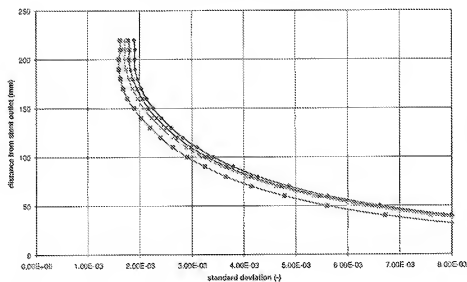


Figure 18: P3 Profile Ridge 8 mm diameter



35 Degree Helix Angle Plot of Swirl Number for Various Graft Lengths

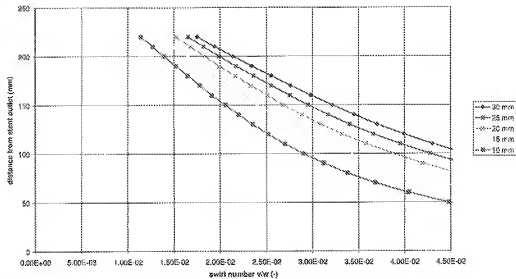


Figure 19: P3 Profile Ridge 8 mm diameter

35 Degree Helix Angle Plot of Standard Deviation for Various Graft Lengths

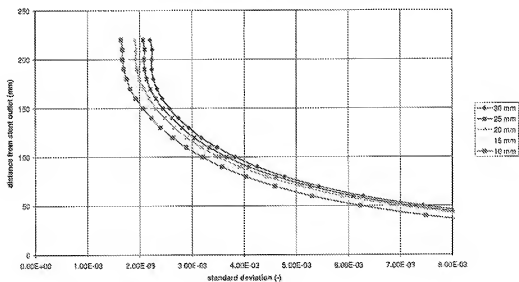


Figure 20: P3 Profile Ridge 8 mm diameter

40 Degree Helix Angle Plot of Swift Number for Various Graft Lengths

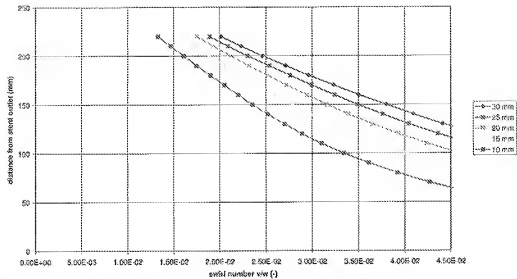


Figure 21: P3 Profile Ridge 8 mm diameter

40 Degree Helix Angle Plot of Standard Deviation for Various Graft Lengths

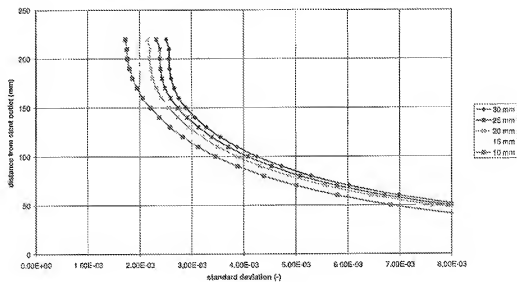


Figure 22: P3 Profile Ridge 8 mm diameter

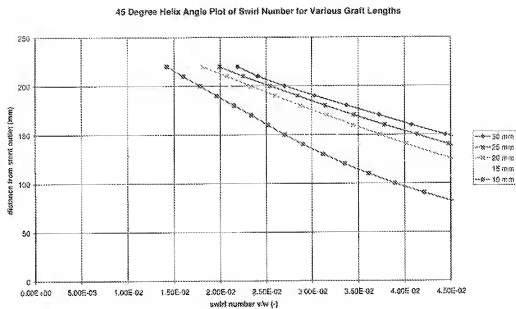


Figure 23: P3 Profile Ridge 8 mm diameter

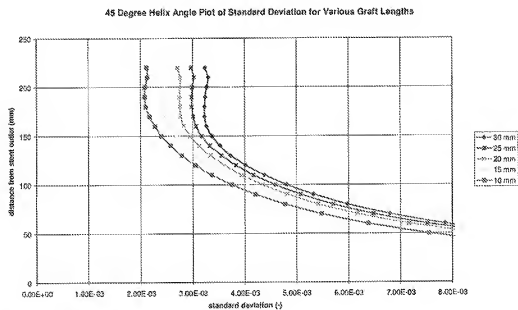


Figure 24: P3 Profile Ridge 8 mm diameter

4 mm x 16 mm Stent Plot of Swirl Number (1 mm)

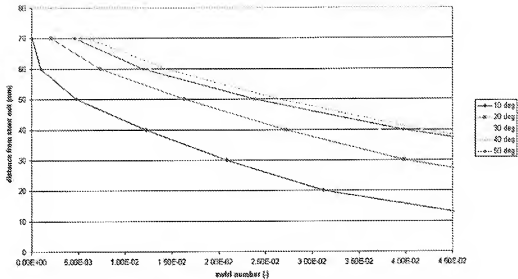


Figure 25: Triangular Ridge Profile (no offset)

4 mm x 16 mm Stent Plot of Standard Deviation (1 mm)

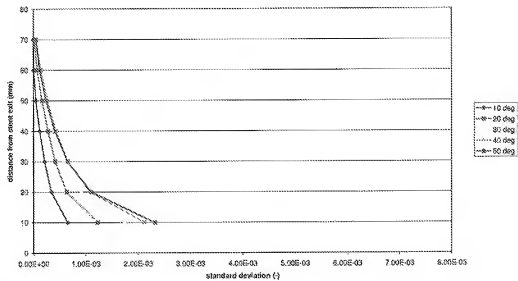


Figure 26: Triangular Ridge Profile (no offset)

4 mm x 15 mm Stent Plot of Swirl Number (0.5 mm)

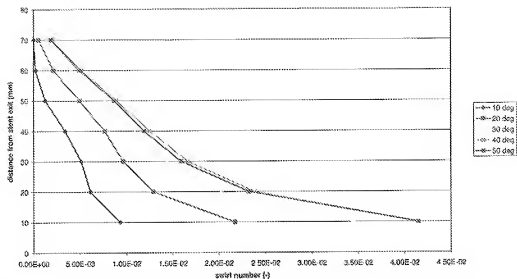


Figure 27: Triangular Ridge Profile (no offset)

4 mm x 15 mm Stent Plot of Standard Deviation (0.5 mm)

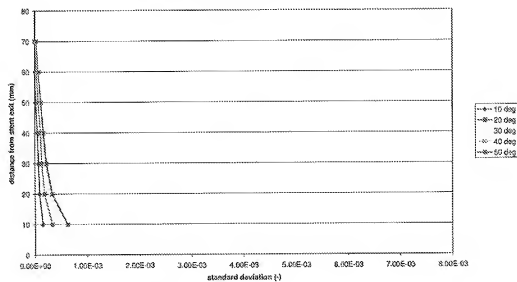


Figure 28: Triangular Ridge Profile (no offset)

3.5 mm x 16 mm Stent Plot of Swirl Number (1 mm)

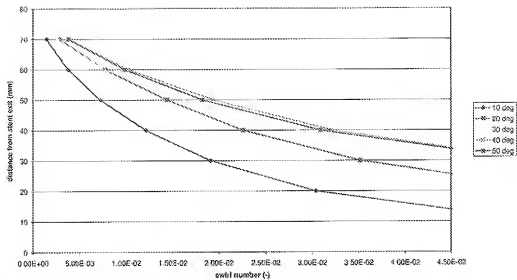


Figure 29: Triangular Ridge Profile (offset)

3.5 mm x 16 mm Stent Plot of Standard Deviation (1 mm)

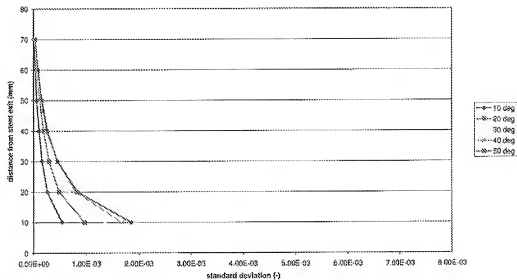


Figure 30: Triangular Ridge Profile (offset)

3.5 mm x 16 mm Stent Plot of Swirl Number (0.5 mm)

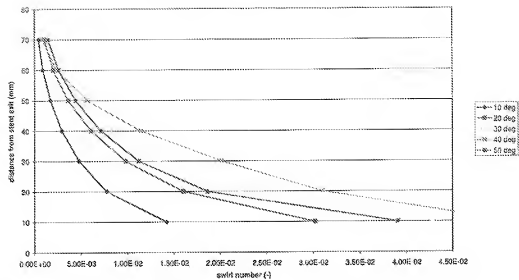


Figure 31: Triangular Ridge Profile (offset)

3.5 mm x 16 mm Stent Plot of Standard Deviation (0.5 mm)

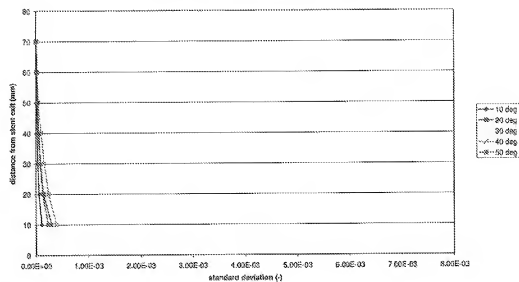


Figure 32: Triangular Ridge Profile (offset)

6 mm x 30 mm Stent Comparison of Different Ridge Shapes

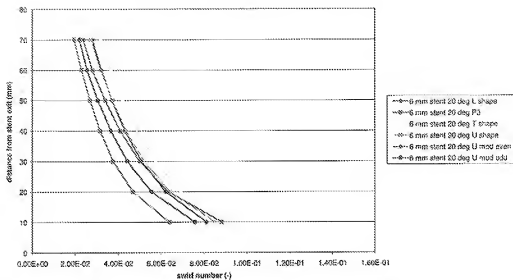


Figure 33: 6 mm Stent Comparison of Ridge Shapes; Swirl Number

6 mm x 30 mm Stent Comparison of Ridge Shapes

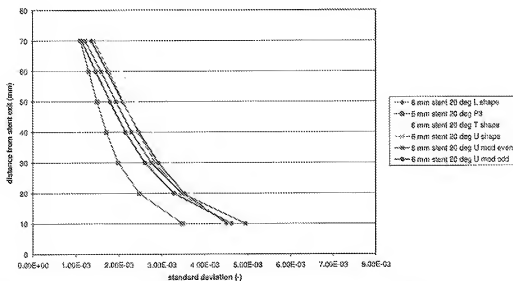


Figure 34: 6 mm Stent Comparison of Ridge Shapes; Standard Deviation



6 mm x 30 mm Stent Comparison of Helical Angles U Shaped Profile

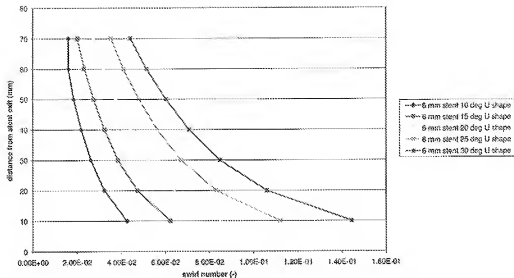


Figure 35: 6 mm Stent Comparison of Helix Angle; Swirl Number

6 mm x 30 mm Stent Comparison of Helical Angles U Shaped Profile

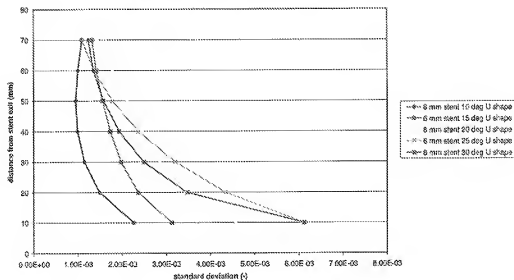


Figure 36: Comparison of Helix Angle; Standard Deviation

8 mm x 30 mm Stent Comparison of Helix Angles for U Shaped Ridge

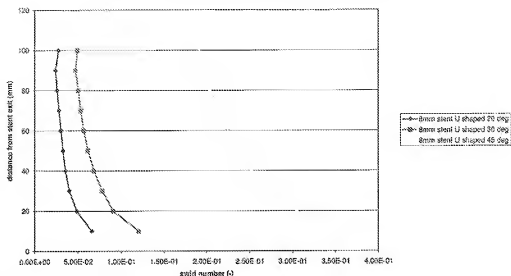


Figure 37: 8 mm x 30 mm Stent U Shaped Ridge; Swirl Number

8 mm x 30 mm Stent Comparison of Helix Angles for U Shaped Ridge

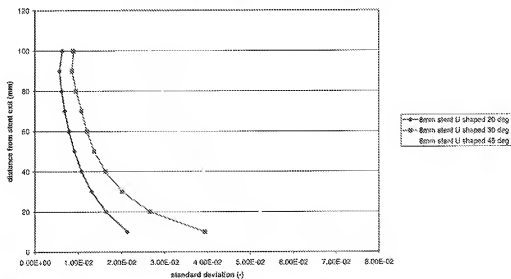


Figure 38: 8 mm x 30 mm Stent U Shaped Ridge; Standard Deviation

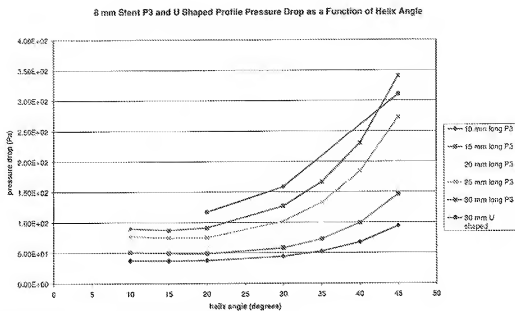


Figure 39: 8 mm Stent P3 and U Shaped Profiles

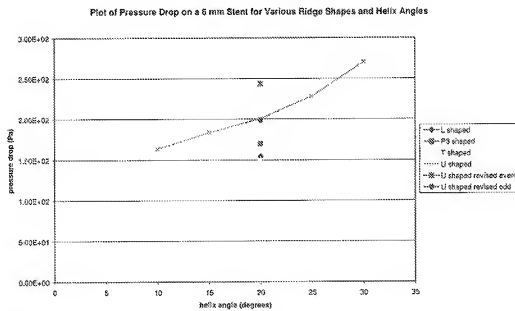


Figure 40: 6 mm Stent Various Ridge Shapes

Plot of Pressure Drop as a Function of Helix angle for 3.5 mm and 4 mm Stents

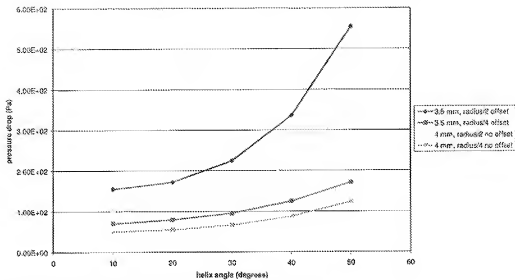


Figure 41: 3.5 mm and 4 mm Stent Triangular Ridge Shape

## ANNEX B

A short study has been carried out to visually compare flow profiles through a 6 mm diameter, 30 mm long stent for various ridge shapes. The results are shown in Appendix B, Figs 1-16.

The swirl number and standard deviation were also calculated on a plane perpendicular to the flow direction, 50 mm from the end of the stent. The results are given below in Table 1.

ridge shape, helix angle	U 30	U 25	U 20	U 15	U 10	T 20	P3 20	L 20
swirl no	0.060262	0.047945	0.0373	0.027568	0.018569	0.042186	0.02707	0.0372
stand dev	0.001578	0.0014	0.001217	0.001016	0.000792	0.001269	0.000953	0.00122

**Table 1: Swirl Number and Standard Deviation at 50 mm Downstream**

Qualitative assessment of transverse velocity profiles:

- The P3 shows less marked high velocities on front face or backface of profile compared to U or T.
- The U shows increased high velocities ("shedding") at the front fin on increasing angle.
- The T shows more marked "shedding" than the U profile.

# APPENDIX 2

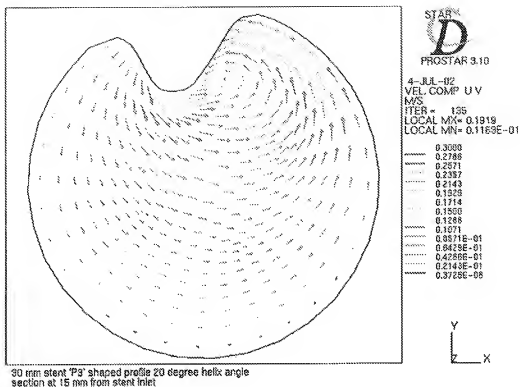


Figure 42

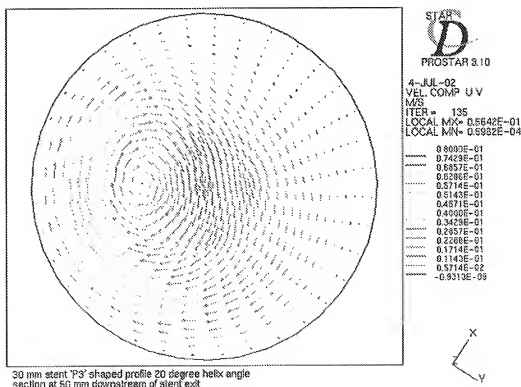


Figure 43

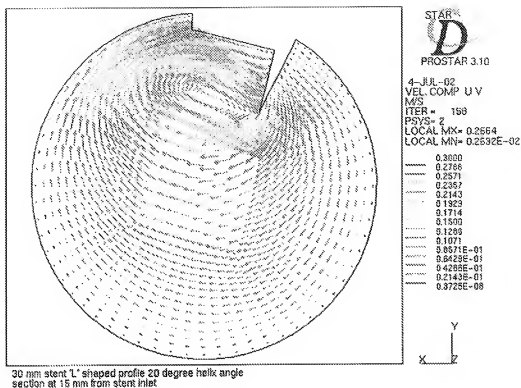


Figure 44

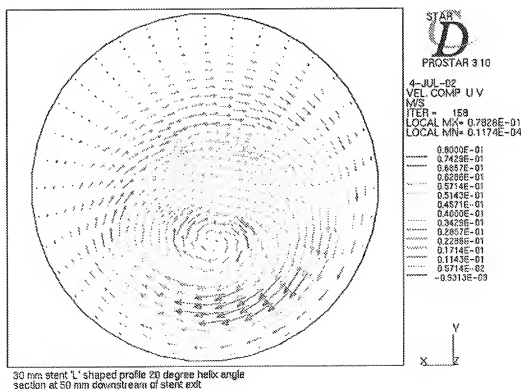


Figure 45

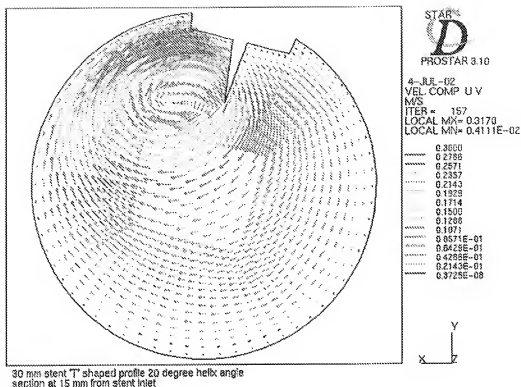


Figure 46

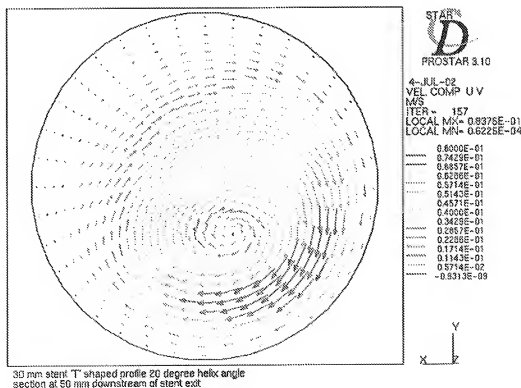


Figure 47



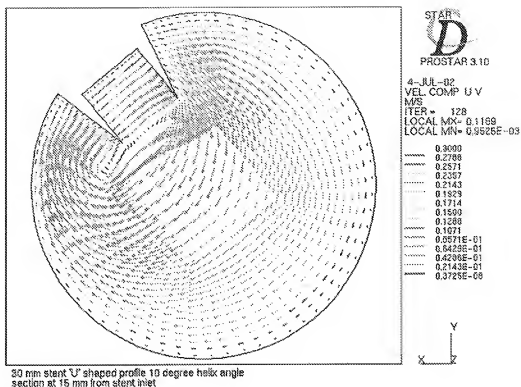


Figure 48

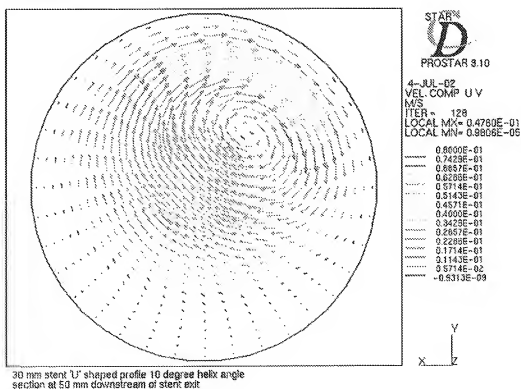


Figure 49

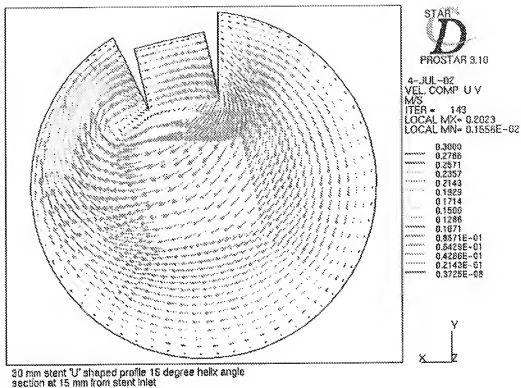


Figure 50

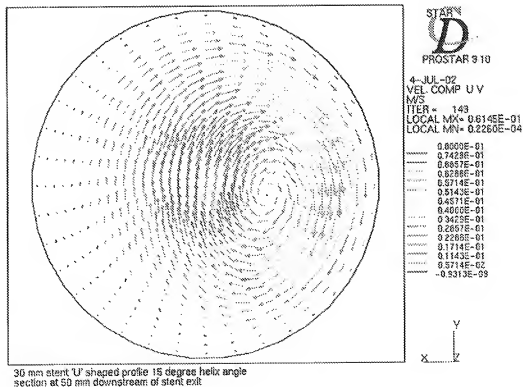


Figure 51

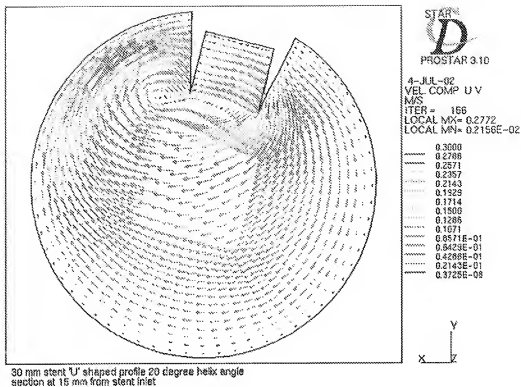


Figure 52

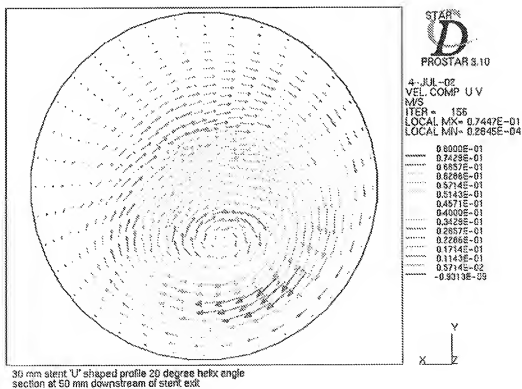


Figure 53

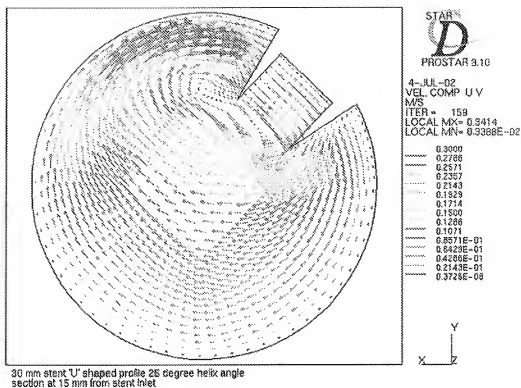


Figure 54

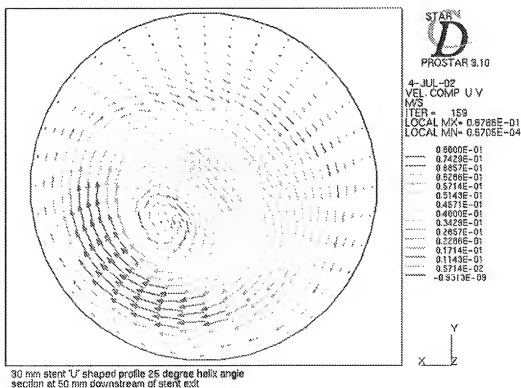


Figure 55

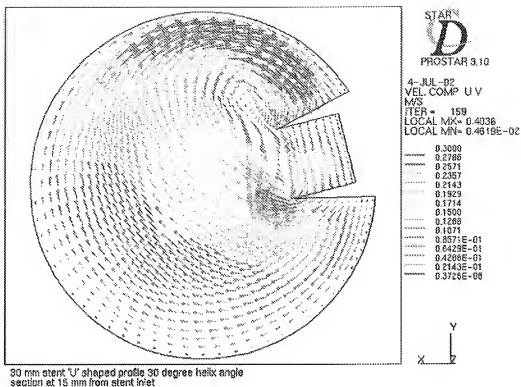


Figure 56

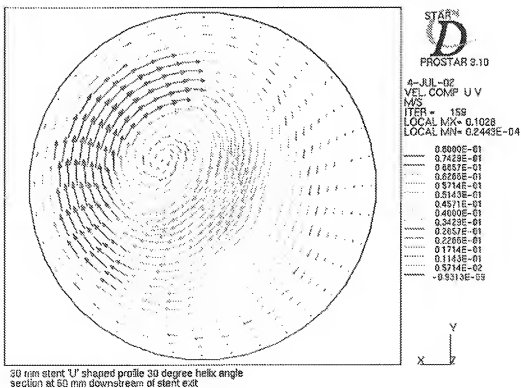


Figure 16

# CURRICULUM VITAE

**NAME** JOHN GRAEME HOUSTON  
**DATE OF BIRTH** 15<sup>th</sup> May 1961  
**PLACE OF BIRTH** Paisley, Scotland

## UNIVERSITY EDUCATION

Magdalene College, CAMBRIDGE	1980-1983
King's College, LONDON	1983-1984
St. Thomas's Hospital, LONDON	1984-1987

## RADIOLOGY TRAINING

Registrar	Western Infirmary Glasgow
Senior Registrar	Western Rotation Glasgow
Interventional Radiology Fellowship	1994-1995
	Vancouver Hospital, UBC site
	British Columbia, Canada

## DEGREES

BA Natural Sciences (Cantab First Class Hons)	1983
Final Year: Pathology, Pharmacology	
MB BChir. (Cantab)	1987
MA (Cantab)	1987
MRCP(UK)	1990
FRCR	1993
MD	1999
FRCP(Ed)	2000

## PRESENT POST

Consultant Radiologist (NHS Tayside)	1995-2009
Chair of Clinical Imaging	2009-
(Honorary Consultant Radiologist NHS Tayside)	

## MEMBERSHIP OF LEARNED SOCIETIES

Royal College of Physicians of Edinburgh.  
Royal College of Radiologists, British Society of Interventional Radiologists.  
Society of Interventional Radiologists (USA).  
Radiological Society of North America.  
International Society of Magnetic Resonance in Medicine.

## POSTS OF RESPONSIBILITY

Tayside Academic Health Sciences Centre Imaging Lead  
Tayside MRI Lead Clinician

### **Budgetary Responsibilities**

I have been responsible for the following budgets and accounts:

- Tayside MRI Service- staff, consumables
- Radiology Research and Training
- Revenue and expenditure equipment, staff
- Research Grant management
- Scottish MRI Seminars co-ordinator
- Interventional Radiology Training Unit for Scotland

### **RESEARCH RECORD**

My main interests are Cardiovascular disease, Image Guided Therapy and Magnetic Resonance Imaging. I have continuing collaborations within the University of Dundee in many clinical and basic science departments, including Surgery and Molecular Oncology, Mechanical Engineering, Surgical Technology Group, TVi within Duncan of Jordanstone. Externally I have collaborations with Aberdeen, Edinburgh and Glasgow Universities.

The main foci of current research are:

- **MRI in cardiovascular disease** including renovascular disease and cardiac failure.
- **Applications of blood haemodynamics to cardiovascular disease**, particularly in relation to vascular graft, stent and heart valves.
- **3-D Visualisation** techniques based on advanced image post-processing to enhance patients understanding of disease, to assist in medical student training, radiotherapy planning and surgical planning.

### **RESEARCH AND DEVELOPMENT EXPERIENCE**

National /International Presentations	120
Published Papers	22
First Author	20
Co-author	5
Invited Review Presentations	3
Book Chapters	34
Patents granted (UK, US , EU)	16
Patents (under application)	